# Determinants of the Broad Recognition of Exocytic Rab GTPases by Mss4†

Zhongyuan Zhu, Anna Delprato, Eric Merithew, and David G. Lambright*

*Program in Molecular Medicine and Department of Biochemistry & Molecular Pharmacology, University of Massachusetts Medical School, Worcester, Massachusetts 01605*

*Received August 17, 2001; Revised Manuscript Received October 10, 2001*

ABSTRACT: Rab GTPases function as essential regulators of vesicle transport between subcellular compartments of eukaryotic cells. Mss4, an evolutionarily conserved Rab accessory factor, facilitates nucleotide release and binds tightly to the nucleotide-free form of exocytic but not endocytic Rab GTPases. A structure-based mutational analysis of residues that are conserved only in exocytic Rab GTPases reveals three residues that are critical determinants of the broad specificity recognition of exocytic Rab GTPases by Mss4. One of these residues is located at the N-terminus of the switch I region near the nucleotide binding site whereas the other two flank an exposed hydrophobic triad previously implicated in effector recognition. The spatial disposition of these residues with respect to the structure of Rab3A correlates with the dimensions of the elongated Rab interaction epitope in Mss4 and supports a mode of interaction similar to that of other exchange factor−GTPase complexes. The complementarity of the corresponding interaction surfaces suggests a hypothetical structural model for the complex between Mss4 and Rab GTPases.

Rab GTPases represent the largest branch of the Ras superfamily, with 11 Rab homologues in budding yeast and at least 60 Rab proteins encoded in the human genome (*1*). Like other GTPases, Rab proteins switch between active (GTP-bound)[1] and inactive (GDP-bound) conformations in a highly regulated GTPase cycle. Guanine nucleotide exchange factors (GEFs) catalyze GDP release and subsequent GTP binding by stabilizing the nucleotide-free state (*2*−*8*). Once activated, Rab GTPases interact with a diverse array of effectors to regulate vesicle budding, cargo sorting, and intracellular transport, as well as the tethering, docking, priming, and fusion of vesicles with acceptor membranes (*9*−*13*). Subsequent inactivation is controlled by GTPase activating proteins (GAPs), which stimulate a weak intrinsic GTP hydrolytic activity (*14*−*17*). The structural differences between the active and inactive forms of Rab GTPases are localized to two conformational switch regions analogous to the switch I and II regions of Ras (*18*). The $\gamma$ phosphate of GTP is detected by direct contacts with an invariant threonine residue in the switch I region and an invariant glycine residue in the switch II region. The active conformation is further stabilized by an extensive hydrophobic interface between the switch I and II regions and through additional interactions with the $\gamma$ phosphate mediated by partially conserved serine residues in the switch I and P-loop regions (*19, 20*).

The interaction of Rab GTPases with regulatory factors and effectors reflects multiple levels of specificity. The majority of known Rab exchange factors, GAPs, and effectors exhibit a high degree of specificity toward Rab GTPases, consistent with the diverse regulatory mechanisms required for the function of Rab GTPases in distinct trafficking pathways. Rab GDI, on the other hand, broadly recognizes members of the Rab family but not other GTPase families (*21*). Several Rab accessory factors exhibit an intermediate level of specificity for distinct Rab subfamilies (*22*−*25*). The high specificity of Rab effector interactions is reflected in the sequence diversity characteristic of the Rab family and determined in part by hypervariable 'Rab complementarity determining regions' (Rab CDRs), which include the N- and C-termini of the GTPase domain as well as the $\alpha 3/\beta 5$ loop (*26*−*28*). An indirect mechanism of effector specificity determination involves sequence variability in the hydrophobic core, which is reflected in the active conformation of a triad of invariant hydrophobic residues located at the interface between the switch I and II regions (*29*). Although a phylogenetic analysis indicates strong evolutionary conservation in the sequences of Rab GTPases that function in common trafficking pathways (*30*), little is known about the determinants of Rab subfamily recognition.

Mss4 (mammalian suppressor of Sec4) binds tightly to the nucleotide-free forms of exocytic Rab GTPases but does not interact with endocytic Rab proteins (*4, 31*). Homologues of Mss4 are present in evolutionarily diverse species including both fission and budding yeast, worms, flies, zebra fish,

† This work was supported by a National Institutes of Health Grant (GM 56324) and by a National Institutes of Health Postdoctoral Training Grant to A.D. (NS 07366). D.G.L. is a Leukemia and Lymphoma Society Scholar.

* Correspondence should be addressed to this author at the Program in Molecular Medicine, Two Biotech, 373 Plantation St., Worcester, MA 01605. Tel: (508) 856-6876. Fax: (508) 856-4289. E-mail: David.Lambright@umassmed.edu.

[1] Abbreviations: DTT, dithiothreitol; GAP, GTPase activating protein; GDP, guanosine diphosphate; GTP, guanosine triphosphate; GEF, guanine nucleotide exchange factor; EDTA, ethylenediaminetetraacetic acid; Hepes, 4-(2-hydroxyethyl)piperazine-1-ethanesulfonic acid; mant-GDP, 2′(3′)-bis-*O*-(*N*-methylanthraniloyl)-GDP; NMR, nuclear magnetic resonance; PCR, polymerase chain reaction; PAGE, polyacrylamide gel electrophoresis; P-loop, phosphate binding loop; SDS, sodium dodecyl sulfate; Tris, tris(hydroxymethyl)aminoethane.

10.1021/bi0116792 CCC: $20.00 
Published on Web 11/29/2001

and mammals (*32*). Overexpression of Mss4 or the budding yeast homologue Dss4 (dominant suppressor of Sec4) suppresses the lethal phenotype of temperature-sensitive dominant-negative Sec4 mutants (*3, 4*). Although viable, a Dss4 null exhibits a synthetic negative phenotype when combined with a temperature-sensitive mutant of Sec2, an essential Sec4 exchange factor (*33*). Mss4 is broadly expressed in different tissues but is most abundant in the brain and is one of the few factors that stimulates neurotransmitter release when injected into squid giant nerve terminals (*31*). These observations implicate Mss4 proteins as Rab accessory factors that regulate exocytosis in cooperation with more potent Rab GEFs (*33*−*35*). Aberrant overexpression of Mss4 has been reported in a wide variety of malignant tissues, including human pancreatic and colon cancers, suggesting a potential role in cancer progression through enhanced secretion of trophic factors required for tumor proliferation and maintenance (*36*).

Studies employing Rab3A/Rab5 chimeras demonstrate that the determinants of the broad recognition of exocytic Rab proteins by Mss4 reside within the N-terminal third of the GTPase domain, which includes the P-loop as well as both conformational switch regions (*24*). Within this region, exocytic Rab GTPases conserve a number of residues that are variable in endocytic Rabs. Several of these residues have been implicated in intramolecular interactions and thus may be conserved for functions other than Mss4 recognition (*19*). For example, serine residues in the P-loop and switch I region of exocytic Rab GTPases regulate the intrinsic and, potentially, the GAP-accelerated rates of GTP hydrolysis through hydrogen bonding interactions with the $\gamma$ phosphate of GTP (*19, 20, 37, 38*). Consequently, it is not clear which of the residues conserved in exocytic Rab GTPases comprise the determinants for broad specificity recognition by Mss4.

To identity Mss4 recognition determinants, eight of the residues selectively conserved in exocytic Rab GTPases were examined in a structure-based mutational analysis of the interaction between Mss4 and Rab3A. The mutants do not show significant effects on the rate of intrinsic nucleotide release. Five mutants exhibited Mss4-catalyzed release activities comparable to or greater than the wild-type protein whereas three residues were found to be critical determinants of the interaction with Mss4. Two of the critical recognition determinants lie within a consensus GEF interaction epitope derived from the crystal structures of four mammalian GEF−GTPase complexes whereas the residues that exhibit the least significant defects when mutated lie outside the consensus epitope. The location of the critical residues with respect to the Rab3A structure suggests a plausible model for the mode of engagement with Mss4 that is consistent with mutational data for both proteins as well as the dimensions and electrostatic properties of the interaction epitopes.

## MATERIALS AND METHODS

*Constructs and Site-Specific Mutagenesis*. Constructs corresponding to residues 14−186 of Rab3A, 9−123 of Mss4, 4−171 of Ypt1, and 16−184 of Sec4 were amplified with Vent polymerase (NEB), digested with *Bam*HI/*Sal*I, and ligated into modified pET15 vectors containing either an N-terminal 6×His tag (Mss4, Ypt1, and Sec4) or an N-terminal 10×His tag followed by a thrombin cleavage site (Rab3A). The Rab constructs correspond to the GTPase domain and lack the hypervariable N- and C-terminal extensions while the Mss4 construct lacks the variable N-terminal extension that is poorly ordered in the NMR structure (*39*). The truncated Mss4 and Rab3A constructs exhibit nucleotide release kinetics that are indistinguishable from the full-length proteins (*32*). Therefore, we will refer to these constructs as Rab3A and Mss4, respectively. Mutations in Rab3A were generated by overlap PCR as described (*32*). All constructs were sequenced from both ends to ensure the absence of secondary mutations.

*Expression and Purification*. BL21(DE3) cells transformed with modified pET15b vectors containing the Mss4 or Rab constructs were grown at 37 °C in 2×YT to an $OD_{600}$ of 0.6−1.0. Protein expression was induced by addition of 1 mM IPTG for 3 h at 37 °C. The cells were resuspended in lysis buffer (50 mM Tris, pH 8.0, 0.1% mercaptoethanol), disrupted by sonication, and centrifuged for 40 min at 35000*g*, and the supernatant was loaded onto a Ni-NTA-agarose column (Qiagen). After being washed with 10 column volumes of 50 mM Tris, pH 8.0, 500 mM NaCl, 10 mM imidazole, 0.1% mercaptoethanol, the fusion proteins were eluted with a gradient of 10−150 mM imidazole (Mss4, Ypt1, and Sec4) or 10−500 mM imidazole (Rab3A) in 50 mM Tris, pH 8.0, 100 mM NaCl, 0.1% mercaptoethanol. The proteins were further purified by ion exchange chromatography on Source Q (Mss4, Ypt1, and Sec4) and by gel filtration on Superdex 75 (all proteins). For Rab GTPases, the buffers were supplemented with 0.5 mM $MgCl_2$.

*Nucleotide Release Assays*. Wild-type and mutant Rab3A proteins were loaded with the fluorescent GDP analogue 2′-(3′)-bis-*O*-(*N*-methylanthraniloyl)-GDP (mant-GDP, Molecular Probes) as described (*32*) and diluted to 50 nM in 20 mM Hepes, pH 8.0, 150 mM NaCl, 0.5 mM $MgCl_2$. The kinetics of nucleotide dissociation were determined by monitoring the decrease in fluorescence associated with the release of mant-GDP. Nucleotide release reactions were initiated by addition of 1 mM GTP and varying concentrations of Mss4. Data were collected on an ISS spectrofluorometer with the excitation wavelength set to 360 nm and the emission monitored at 440 nm. Observed pseudo-first-order rate constants ($k_{obs}$) at each concentration of Mss4 were extracted from a nonlinear least-squares fit to the exponential function:

$$I(t) = (I(0) - I(\infty)) \exp(-k_{obs}t) + I(\infty) \qquad (1)$$

For each time course, data were collected until $I(t)$ had decayed to within 5% of $I(\infty)$, which corresponds to at least 3 times the value of $1/k_{obs}$. Apparent $k_{cat}$ and $K_m$ values were determined from a nonlinear least-squares fit to the Michaelis−Menten function:

$$k_{obs} = k_{cat}[\text{Mss4}]/(K_m + [\text{Mss4}]) + k_{intr} \qquad (2)$$

where $k_{intr}$ represents the intrinsic rate of nucleotide release, which was fixed at the measured value for each mutant.

The average standard deviation in $k_{obs}$ calculated from 2−4 replicate measurements is ∼10%. However, due to the severity of the defects in $K_m$ for several of the mutants, the kinetic data are incomplete at high concentrations of Mss4. Consequently, the uncertainty in the estimation of the kinetic

parameters considerably exceeds the statistical error in $k_{obs}$. Therefore, error ranges that include the larger uncertainty in the parameter estimation were determined by allowing either $k_{cat}$ or $K_m$ to adjust freely while systematically incrementing the fixed parameter in both directions until chi-squared was twice that obtained when both $k_{cat}$ or $K_m$ were treated as freely adjustable parameters. The values of the fixed parameter at the lower and upper bounds where chi-squared equals twice the fitted minimum correspond to a confidence interval of 68.3% (*40*) and are listed as the limits of the estimated error range in Table 1. An analogous procedure was used to determine the error range for the catalytic efficiency ($k_{cat}/K_m$). The relative uncertainty in $k_{cat}/K_m$, which corresponds to the slope of eq 2 at low concentrations of Mss4, is much less than that of the individual parameter values. Consequently, $k_{cat}/K_m$ provides a reliable indicator of the effects of the mutations, regardless of their magnitude.

*Gel Filtration Experiments*. Stable nucleotide-free complexes between Mss4 and exocytic Rab GTPases were prepared by mixing stoichiometric quantities of the proteins at a total concentration of 10 mg/mL in 50 mM Tris, pH 8.0, 4 mM DTT, and 1 $\mu$g/mL activated charcoal (HCl washed, Sigma). After incubating overnight at 4 °C, the solutions were passed through a 0.2 $\mu$m acrodisc filter and loaded onto a Superdex 75 or a Superdex 200 column (Pharmacia) equilibrated with 10 mM Tris, pH 8.0, 0.2 M NaCl, and 0.1% 2-mercaptoethanol. The columns were calibrated using ribonuclease A (13.7 kDa), chymotrypsinogen A (25 kDa), ovalbumin (43 kDa), and bovine serum albumin (67 kDa). The protein composition of each peak was determined by SDS−PAGE (data not shown).

## RESULTS

A structure-based alignment of representative Rab sequences (Figure 1A) reveals a subset of residues that are highly conserved in exocytic Rab GTPases but variable in the endocytic subfamily. Most of these residues fall within the N-terminal third of Rab3A (residues 1−102) previously implicated in the interaction with Mss4 and cluster in or near the P-loop and switch regions (*24*). Mutational and crystallographic studies of the interactions between other monomeric GTPases and their cognate GEFs have highlighted the importance of residues in the P-loop and switch regions (*41*−*45*). The majority of the residues selectively conserved in exocytic Rab GTPases occupy exposed or partially exposed positions in the structure of GppNHp-bound Rab3A (*19*). It is likely that at least some of the residues conserved in exocytic Rab GTPases contribute directly to the interaction with Mss4. To identify determinants of the broad recognition of exocytic Rab GTPases by Mss4, eight of the selectively conserved residues (Ser 31, Asp 45, Phe 51, Val 52, Ser 53, Lys 60, Val 61, and Thr 89) were targeted for mutational analysis. The location of these residues with respect to the Rab3A structure and known functional regions is shown in Figure 1B. To avoid complex phenotypes, the selected residues were converted to alanine, which occurs naturally at each position in at least one Rab GTPase and is therefore unlikely to disrupt the structure of the protein. Consistent with this expectation, all mutants expressed in soluble form at wild-type levels and exhibited no observable defects during purification, with the exception of the D45A mutant, which formed higher order oligomers as detected by gel filtration (see below).

The intrinsic and Mss4-stimulated rates of nucleotide dissociation were determined by loading wild-type or mutant Rab3A proteins with the fluorescent GDP analogue mant-GDP and monitoring the decrease in fluorescence that accompanies the release of mant-GDP in the presence of a large excess of GTP. Mutants that significantly perturb the structure would be expected to exhibit defects in the intrinsic rate of nucleotide release. As anticipated, the intrinsic rate of nucleotide release for all eight mutants was very similar to that of the wild-type protein (Table 1), indicating that the mutants maintain a stable structure similar to that of wild-type Rab3A.

The ability of Mss4 to catalyze release of mant-GDP from the various mutants was initially assessed at a concentration of Mss4 equivalent to the $K_m$ for the wild-type protein. Representative data for the wild-type protein and four mutants are shown in Figure 2A. Whereas some mutants exhibited a severe defect, others showed enhanced rates of nucleotide release. To gain further insight into the kinetic properties of the mutant proteins, exchange assays were conducted at various concentrations of wild-type Mss4. The observed pseudo-first-order rate constants were plotted as a function of Mss4 concentration (Figure 2B−D) and the apparent $K_m$ and $k_{cat}$ parameters extracted from a fit to a Michaelis−Menten kinetic model (eq 2). The resulting kinetic constants for all eight mutants are summarized in Table 1.

Based on the observed kinetic properties, the mutants can be divided into distinct groups. Mutants F51A,V61A, and T89A exhibit severe defects, with greatly increased $K_m$ and, possibly, decreased $k_{cat}$. Due to the magnitude of the defect for these mutants, an accurate assessment of the individual kinetic constants is precluded. However, the catalytic efficiency ($k_{cat}/K_m$) is well determined and provides a useful measure of the severity of the defects. In contrast, mutants S31A and K60A showed relatively modest defects in either $k_{cat}$ or $K_m$ while three other mutants (D45A, V52A, and S53A) exhibited either increased $k_{cat}$ or decreased $K_m$. D45A significantly decreased $K_m$ with little effect on $k_{cat}$, leading to a 5-fold increase in $k_{cat}/K_m$. V52A and S53A, on the other hand, exhibited a 2−4-fold increase in $k_{cat}$; however, due to a corresponding increase in $K_m$, the net effect on $k_{cat}/K_m$ was negligible.

Although Mss4 forms stable 1:1 complexes with Rab3A, minor peaks on gel filtration indicate the presence of higher order oligomers with estimated stoichiometries of 2:2 and 3:3 (Figure 3). To further explore the interaction between Mss4 and Rab proteins, nucleotide-free complexes of Mss4 and various Rab GTPases were prepared and isolated by gel filtration chromatography. Mss4 also forms stable 1:1 complexes with both Sec4 and Ypt1, with little evidence of higher order aggregation. Interestingly, however, the D45A mutant forms a stable complex that elutes near the void volume on Superdex-75. Subsequent chromatography on Superdex-200 yields a single peak with an apparent molecular mass of ~130 kDa, consistent with 4:4 stoichiometry. In the absence of Mss4, Rab3A, Sec4, and Ypt1 elute as monomers whereas the majority of the D45A mutant elutes with an apparent molecular weight of either a tetramer or a higher order aggregate. The propensity of the D45A mutant

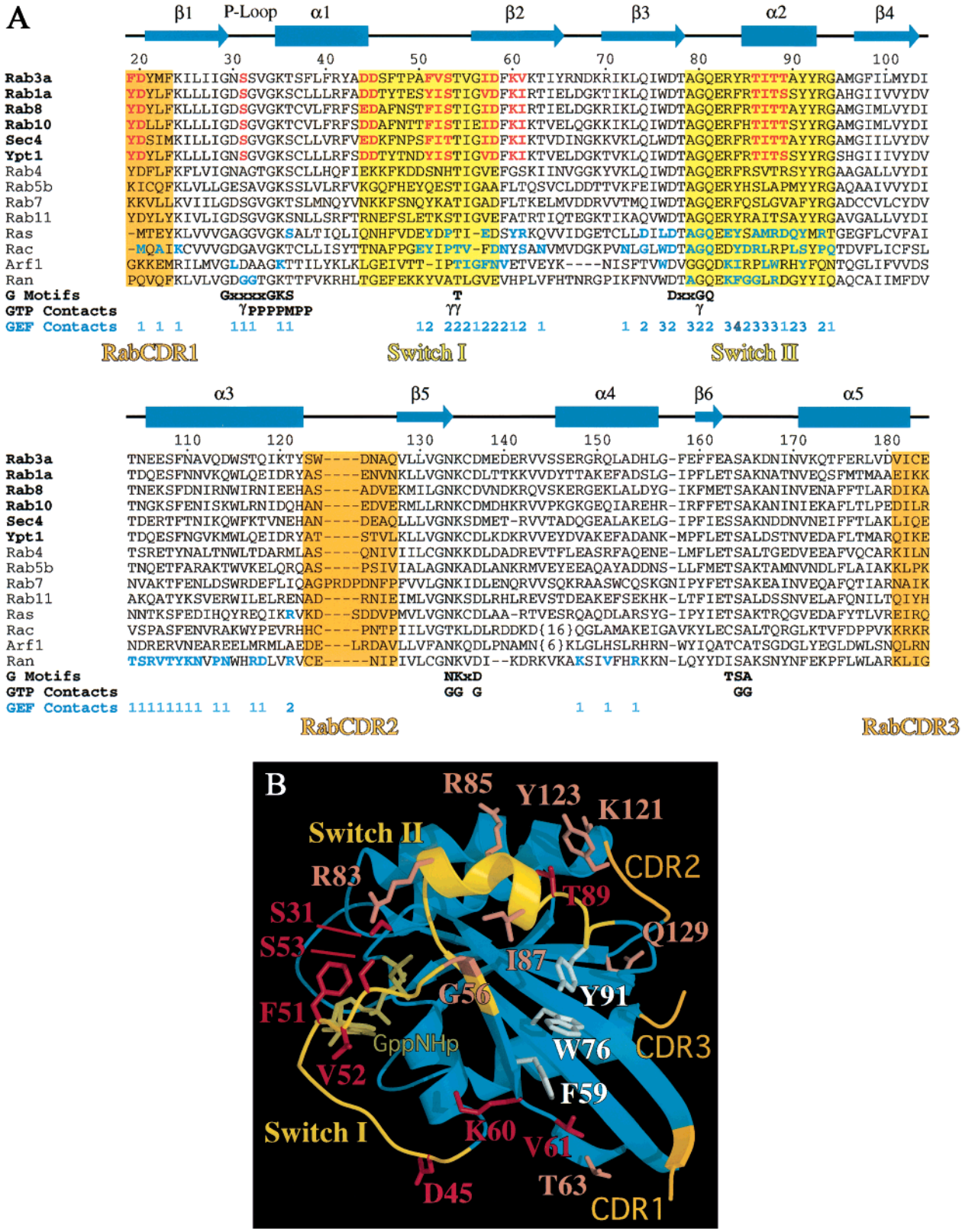


FIGURE 1: Selection of putative recognition determinants for mutational analysis. (A) Structure-based sequence alignment of representative Rab family and related GTPases. Exocytic Rab proteins are indicated by boldface type. Residues that are highly conserved in the exocytic Rab subfamily but variable in endocytic Rab GTPases are highlighted in red. Residues highlighted in blue participate in direct GEF contacts in the crystal structures of Ras-Sos, Arf1-Sec7, Rac-Tiam1, and Ran-RCC1 (*42*−*45*). The number of GEF contacts at each position is indicted below the alignment. (B) Location of conserved and mutated residues with respect to the crystal structure of GppNHp-bound Rab3A (*32*). Residues truncated to alanine in the present study are shown in dark red whereas residues implicated in the interaction between Dss4 and Ypt1 (*46*) are shown in light red. Note that Thr 89 was also implicated in the latter study. Invariant residues shown in white comprise the partially exposed hydrophobic triad located at the interface of the switch I and II regions of Rab GTPases.

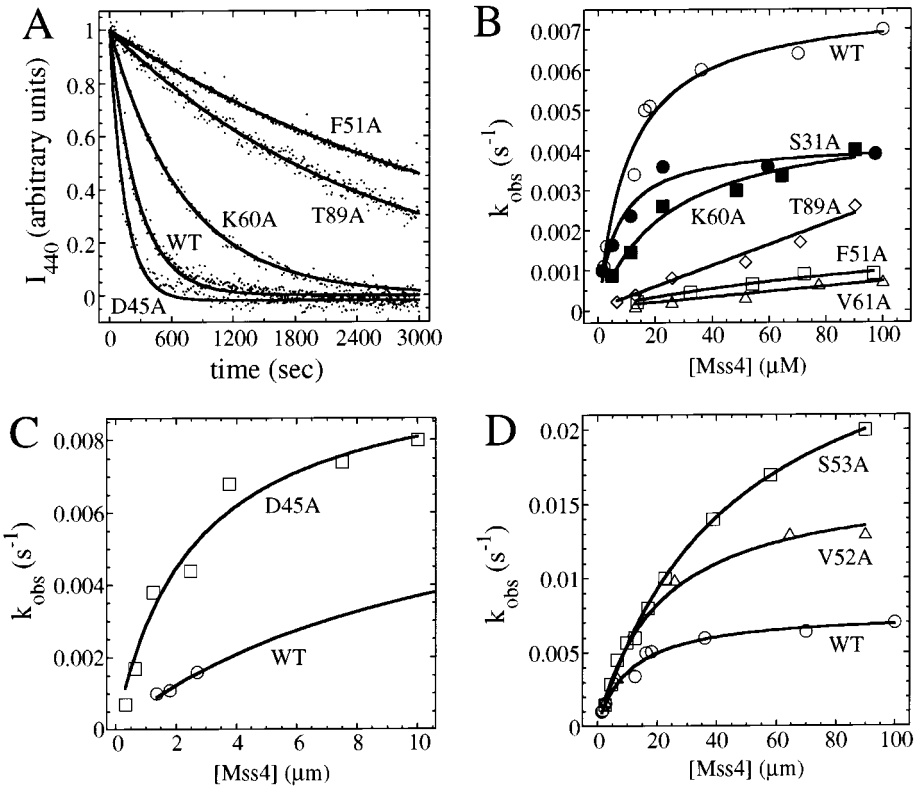


FIGURE 2: Exchange kinetics for Rab3A mutants. (A) Normalized fluorescence time course for the dissociation of mant-GDP from Rab3A mutants (F51A, T89A, D45A, and K60A) or wild-type (WT) Rab3A in the presence of 13.5 $\mu$M Mss4. Solid lines represent the fitted exponential time courses from which pseudo-first-order rate constants were extracted (see Materials and Methods). (B−D) Observed pseudo-first-order rate constants ($k_{obs}$) as a function of Mss4 concentration. Solid lines represent fitted model functions for the dependence of the observed rate constants on the concentration of Mss4 (see Materials and Methods).

Table 1: Summary of Kinetic Parameters for Mss4 Mutants

| protein | $k_{intrinsic}$ ($\times 10^{-5}$ $s^{-1}$) | $k_{cat}$[a] ($\times 10^{-3}$ $s^{-1}$) | error range[b] | $K_m$[a] ($\times 10^{-6}$ M) | error range[b] | $k_{cat}/K_m$[a] ($M^{-1}$ $s^{-1}$) | error range[b] | $(k_{cat}/K_m^{mut})/(k_{cat}/K_m^{wt})$ |
|---|---|---|---|---|---|---|---|---|
| wild type | 7.5 | 7.7 | 6.8−8.6 | 11 | 7.5−16 | 715 | 500−970 | 1 |
| S31A | 7.2 | 4.1 | 3.6−4.8 | 7.0 | 4−12 | 590 | 390−950 | 0.83 |
| D45A | 8.0 | 10 | 8.4−13 | 2.6 | 1.6−4.3 | 3900 | 2700−5600 | 5.4 |
| F51A | 5.4 | 2.4 | 1.4−13 | 170 | 70−1400 | 14 | 11−22 | 0.020 |
| V52A | 4.8 | 17 | 15−17 | 21 | 15−30 | 800 | 620−1050 | 1.1 |
| S53A | 5.4 | 30 | 27−33 | 45 | 38−55 | 660 | 600−740 | 0.92 |
| K60A | 14 | 4.7 | 4.1−5.8 | 25 | 16−44 | 190 | 130−250 | 0.27 |
| V61A | 9.7 | 1.8 | 1−12 | 180 | 95−1200 | 10 | 3.9−23 | 0.014 |
| T89A | 8.8 | 5 | 3−18 | 150 | 85−600 | 33 | 21−44 | 0.032 |

[a] Best-fit parameter values obtained from the data in Figure 2B−D (see Materials and Methods). [b] Error range corresponds to the 68.3% confidence interval (equivalent to one standard deviation of a normal distribution) and includes measurement error as well as uncertainty in the estimation of parameters due to parameter correlation and incomplete data at high concentrations of Mss4 (see Materials and Methods).

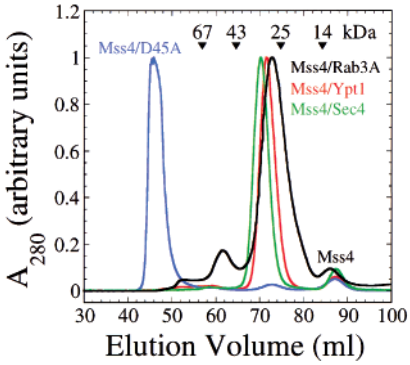


FIGURE 3: Isolation of nucleotide-free Mss4−Rab complexes by gel filtration on Superdex-75. Elution volumes for globular molecular weight standards are indicated above the chromatograms.

to form higher order oligomers in both the presence and absence of Mss4 presumably accounts for the decrease in $K_m$ observed in the D45A mutant.

The distal spatial relationship of the three critical recognition determinants provides insight into the structural elements of exocytic Rab GTPases that mediate the interaction with Mss4. As shown in Figure 1, Phe 51 lies at the N-terminus of the switch I region, near the phosphate and $Mg^{2+}$ binding site, whereas Val 61 is located in the $\beta$2 strand, just beyond the C-terminus of the switch I region, while Thr 89 resides at the C-terminus of the α2 helix in the switch II region. Although Phe 51 and Val 61 are completely exposed, Thr 89 is only partially exposed in the GTP-bound form. Structural data are not available for the GDP-bound form of Rab3A; however, the corresponding residues in the GDP-

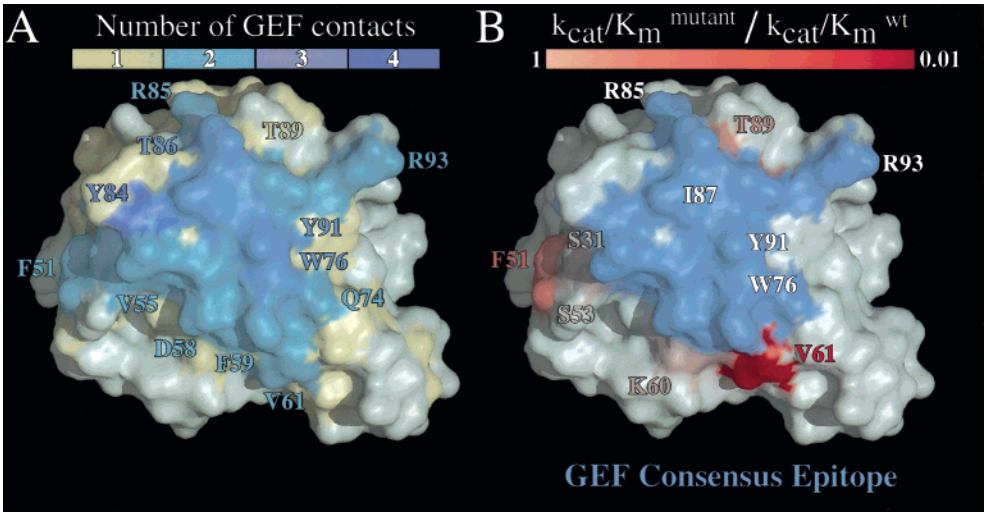


FIGURE 4: Distribution of critical Mss4 recognition determinants with respect to the crystal structure of GppNHp-bound Rab3A (*32*). (A) Extent of overlap in GEF interaction epitopes deduced from the crystal structures of Ras-Sos, Arf1-Sec7, Rac-Tiam1, and Ran-RCC1 (*42*−*45*) and mapped onto the surface of Rab3A. (B) Location and relative contribution of Mss4 recognition determinants. The relative change in catalytic efficiency resulting from alanine substitution is highlighted from minor (light red) to severe (dark red) defects. Blue denotes the GEF consensus epitope defined as two or more GEF contacts.

bound form of Sec4 (the Rab3A homologue in budding yeast) are either exposed or disordered (*18*). Consequently, the simplest interpretation is that Phe 51, Val 61, and possibly Thr 89 contribute directly to the interface with Mss4, which presumably explains (at least in part) their conservation in exocytic but not endocytic Rab GTPases. Interestingly, Val 61 and Thr 89 flank an invariant triad of partially exposed aromatic residues (Phe 59, Trp 76, and Tyr 91) located at the hydrophobic interface between the switch I and II regions.

Crystal structures of nucleotide-free EF-Tu, Ras, Arf1, Rac, and Ran have been solved in complex with their cognate GEFs (*42*−*45*). Despite the lack of structural homology between the various GEFs and significant differences in the interaction interfaces, some general principles have emerged. In all cases, the GEFs contact the switch II region as well as the P-loop and/or switch I regions, resulting in structural changes that disrupt interactions with the phosphates and $Mg^{2+}$ ion. The extent of the overlap in the various interaction interfaces can be represented in the form of a 'consensus epitope' obtained by assigning each position in an alignment of GTPase sequences a score equivalent to the number of known structures in which the corresponding residue lies within the GEF interface. In Figure 4A, the consensus epitope derived from the four mammalian GTPase−GEF complexes of known structure (see Figure 1A) is mapped onto the surface of the Rab3A structure. For the numerous nucleotide-free Rab−GEF complexes whose structures have not been determined, we propose that the consensus epitope can be interpreted as a map of the likelihood that any given residue in a Rab GTPase will lie within the GEF interaction interface. As a first step toward validation of this hypothesis, Figure 4B compares the location of the five Rab3A mutants that exhibit defects in $k_{cat}/K_m$ with the GEF consensus epitope. Interestingly, two of the three critical Mss4 recognition determinants identified by mutational analysis (Phe 51 and Val 61) reside within the GEF consensus epitope whereas the three residues that exhibited the weakest effects when mutated (Ser 31, Val 52, and Lys 60) lie outside the GEF consensus epitope.

## DISCUSSION

Eight residues that are highly conserved among exocytic Rab GTPases but variable in endocytic Rab proteins were subjected to mutational analysis. Although it is formally possible that the Rab3A mutations interfere with Mss4 binding as a consequence of global structural defects, several lines of evidence argue against this interpretation. First, all of the residues selected for mutational analysis occupy exposed or partially exposed positions in the GppNHp-bound Rab3A crystal structure (*19*). Second, the intrinsic rate of nucleotide release for all of the mutants is very similar to that of the wild-type protein, indicating that significant structural changes do not occur in the nucleotide binding site. Finally, nonconservative substitutions including alanine are frequently observed at these positions in endocytic Rabs. Thus, any local effect on the structure is likely to contribute to the physiological mechanism for specificity determination.

Of the eight Rab3A residues examined in this study, three (Phe 51, Val 61, and Thr 89) were found to be critical determinants for recognition of exocytic Rab family GTPases by Mss4. Alanine mutants of Ser 31, Val 52, and Lys 60, on the other hand, have relatively minor effects on the interaction with Mss4, suggesting that these residues are likely conserved for an alternative function common to exocytic Rab GTPases. For example, Ser 31 interacts with the $\gamma$ phosphate of GTP and is a negative determinant of the intrinsic GTPase activity (*19*, *38*). The D45A mutant decreases $K_m$ by ~5-fold, with little effect on $k_{cat}$; however, the observation that the D45A mutant forms higher order oligomers as detected by gel filtration chromatography likely accounts for the apparent increased affinity. Even though Asp 45 does not appear to play a direct role in the interaction with Mss4, it may contribute indirectly by reducing the aggregation propensity. Finally, the S53A mutant increases both $k_{cat}$ and $K_m$ by 4-fold but has no significant effect on the intrinsic exchange rate. The increase in $k_{cat}$ fully accounts for the corresponding increase in $K_m$ and implicates the hydroxyl group of Ser 53 in a rate-limiting step of the kinetic mechanism for nucleotide release.

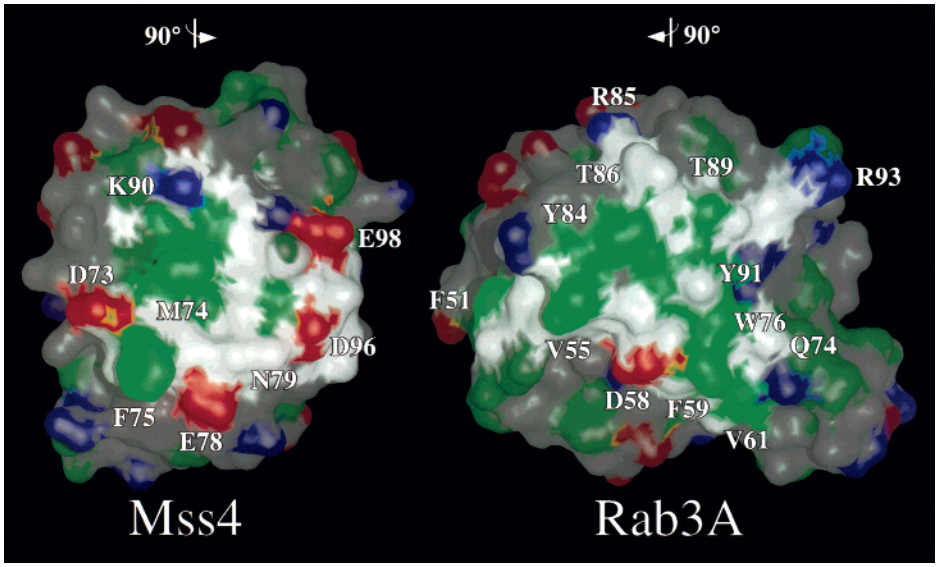


FIGURE 5: Hypothetical model for the interaction of Mss4 and Rab3A consistent with experimental observations. Negatively and positively charged groups are colored red and blue, respectively, whereas nonpolar atoms are colored green. Highlighted surfaces correspond to the conserved Rab interaction epitope of Mss4 and the GEF consensus epitope of Rab3A.

In a screen for intragenic suppressors of a dominant-negative mutant of Ypt1 (the Rab1 homologue in budding yeast), nine site-specific mutants were identified that disrupt the interaction with Dss4 (*46*). The mutated residues are located in the switch I and switch II regions as well as the variable α3−β5 loop of Ypt1. Rab5/Rab3A chimeric mutants indicate that the specificity determinants for interaction with Mss4 reside within residues 1−102 of Rab3A, which does not include the hypervariable α3−β5 loop (*24*), suggesting possible differences in the detailed interactions of Rab proteins with Mss4 and Dss4. Nevertheless, it is noteworthy that mutants of several residues in the switch II region of Ypt1 (equivalent to Arg 83, Arg 85, Ile 87, and Thr 89 in Rab3A) were found to be defective with respect to Dss4-stimulated exchange activity (*46*). Using a structure-based rational approach, we have identified three critical residues in or near the switch I and switch II regions. Only one of the critical residues (Thr 89) was also detected in the second site suppressor screen. Although this might reflect expected differences in the interaction of the various exocytic Rab GTPases with Mss4 and Dss4, an alternative explanation is that some mutants, including those corresponding to Phe 51 and Val 61, were not selected in the second site suppressor screen due to incomplete coverage. An earlier mutational study of Rab3A identified several residues that participate in the interaction with Rab3 GRF, a partially purified high molecular mass GEF activity with specificity for Rab3A (*2*). When compared with the results of the present study, an interesting similarity emerges. Phe 51 and Phe 59, but not Ser 31, were found to be important for the interaction with Rab3A GRF (*37*, *38*). Phe 51 is a critical Mss4 recognition determinant, and the invariant Phe 59 lies adjacent to Val 61 in the Rab3A structure. Thus, it appears that Mss4, Dss4, and Rab3A GRF share significant overlap in their mode of interaction with Rab3A.

A consensus GEF interaction epitope derived from crystal structures of distantly related nucleotide-free GTPases in complex with nonhomologous GEFs provides a convenient framework for assessing the general significance of the mutational data on GEF interactions with Rab GTPases. Two critical determinants for recognition of exocytic Rab GTPases by Mss4 (Phe 51 and Val 61) lie within the GEF consensus epitope as do three of the Ypt1 residues implicated in the interaction with Dss4 (corresponding to switch II residues Arg 85, Ile 87, and Thr 89 in Rab3A) as well as four Rab3A residues found to be important for interaction with Rab3 GRF (Phe 51, Thr 54, Val 55, and Phe 59). Conversely, mutants which exhibited relatively small effects on Mss4-stimulated exchange activity involved residues outside the consensus epitope (Ser 31, Val 52, and Lys 60). Thus, the available crystallographic and mutational data on Rab GTPases strongly support a mode of GEF interactions similar to other GTPase families, suggesting that the GEF consensus epitope will serve as a meaningful likelihood predictor for the large family of Rab GTPases.

Chemical shift perturbations in the presence of Sec4 define a Rab interaction epitope that maps to an evolutionarily conserved subdomain of Mss4 (*32*, *39*). Two critical interaction determinants (Asp 96 and residues $^{73}$DMF$^{75}$ of the DΦΦ motif) are located at opposite ends of the conserved subdomain (*32*). Figure 5 depicts a hypothetical model for the engagement of Rab3a by Mss4 consistent with the mutational data as well as the overall dimensions and electrostatic properties of the putative interaction epitopes. If the hydrophobic residues of the DΦΦ motif of Mss4 are positioned so as to engage Val 61 and the invariant hydrophobic triad of Rab3A, it would be possible for Asp 96 of Mss4 to interact with elements of the P-loop and/or $Mg^{2+}$ binding site. The outer surface of the conserved $Zn^{2+}$ binding site in Mss4 would then be appropriately oriented to contact Phe 51 in Rab3A. Asp 96 of Mss4 exhibits a severe defect when mutated, consistent with the apparently general involvement of acidic residues in the disruption of the $Mg^{2+}$ binding site and P-loop regions of monomeric GTPases by other GEFs (*42*−*45*). This model would also place the βH/βI loop of Mss4 near the variable α3/β5 loop of Rab3A. Dss4 contains a 26 residue insertion in the βH/βI loop, which might explain the paradoxical observation that the α3/β5 loop is important for the interaction of Ypt1 with Dss4 but not for the interaction of Rab3A with Mss4 (*24*, *46*). However, other

models are possible, and a detailed understanding of the interaction and its relationship to other GTPase−GEF systems will require the structure of a complex between Mss4 and an exocytic Rab GTPase.

The role of Mss4 in vivo has yet to be fully understood. It was first identified as a suppressor for a temperature-sensitive Sec4 mutant in yeast and shown to have exchange activity for a number of exocytic Rabs (*4*, *31*). However, Mss4 is not required for the function of Rab1A in endoplasmic reticulum to Golgi transport. Likewise, whereas Sec4 is essential for growth of budding yeast, Dss4 is not, consistent with the involvement of other exchange factors such as Sec2p (*33*, *35*). Moreover, the observed $k_{cat}$ for Mss4 is low compared with several well-characterized GEFs for other GTPases. In view of these observations, Mss4 was proposed to function as a chaperone for misfolded nucleotide-free intermediates that might otherwise accumulate to levels sufficient to exhibit dominant-negative effects by binding tightly to and interfering with the function of specific exchange factors (*35*). We have shown that Mss4 possesses critical structural elements reminiscent of other GEFs and, like its yeast homologue Dss4, engages the switch I and II regions of Rab GTPases (*32*, *46*). Thus, to the extent that Mss4 functions as a chaperone for the nucleotide-free state in vivo, the underlying structural mechanism evidently resembles that of other GEFs, thereby explaining the observed exchange activity toward exocytic Rab GTPases in vitro. However, the observation that a subtle serine to alanine mutation in Rab3A can significantly enhance $k_{cat}$ for Mss4-catalyzed nucleotide release raises the possibility that Mss4 might exhibit higher exchange activity for an as yet unidentified Rab GTPase and/or require additional factors for activation. Further studies are needed to determine the precise cellular role of Mss4 and its potential regulation by accessory proteins.

## ACKNOWLEDGMENT

We thank Janet Burton and Pietro De Camilli for cDNA clones of Mss4 and Rab3A.

## REFERENCES

1. Bock, J. B., Matern, H. T., Peden, A. A., and Scheller, R. H. (2001) *Nature 409*, 839−841.
2. Burstein, E. S., and Macara, I. G. (1992) *Proc. Natl. Acad. Sci. U.S.A. 89*, 1154−1158.
3. Moya, M., Roberts, D., and Novick, P. (1993) *Nature 361*, 460−463.
4. Burton, J., Roberts, D., Montaldi, M., Novick, P., and De Camilli, P. (1993) *Nature 361*, 464−467.
5. Horiuchi, H., Lippe, R., McBride, H. M., Rubino, M., Woodman, P., Stenmark, H., Rybin, V., Wilm, M., Ashman, K., Mann, M., and Zerial, M. (1997) *Cell 90*, 1149−1159.
6. Hama, H., Tall, G. G., and Horazdovsky, B. F. (1999) *J. Biol. Chem. 274*, 15284−15291.
7. Jones, S., Newman, C., Liu, F., and Segev, N. (2000) *Mol. Biol. Cell 11*, 4403−4411.
8. Wang, W., Sacher, M., and Ferro-Novick, S. (2000) *J. Cell Biol. 151*, 289−296.
9. Waters, M. G., and Pfeffer, S. R. (1999) *Curr. Opin. Cell Biol. 11*, 453−459.
10. Somsel Rodman, J., and Wandinger-Ness, A. (2000) *J. Cell Sci. 113 Pt. 2*, 183−192.
11. Armstrong, J. (2000) *Int. J. Biochem. Cell Biol. 32*, 303−307.
12. Carroll, K. S., Hanna, J., Simon, I., Krise, J., Barbero, P., and Pfeffer, S. R. (2001) *Science 292*, 1373−1376.
13. Deacon, S. W., and Gelfand, V. I. (2001) *J. Cell Biol. 152*, F21−F24.
14. Strom, M., Vollmer, P., Tan, T. J., and Gallwitz, D. (1993) *Nature 361*, 736−739.
15. Fukui, K., Sasaki, T., Imazumi, K., Matsuura, Y., Nakanishi, H., and Takai, Y. (1997) *J. Biol. Chem. 272*, 4655−4658.
16. Du, L. L., Collins, R. N., and Novick, P. J. (1998) *J. Biol. Chem. 273*, 3253−3256.
17. Albert, S., Will, E., and Gallwitz, D. (1999) *EMBO J. 18*, 5216−5225.
18. Stroupe, C., and Brunger, A. T. (2000) *J. Mol. Biol. 304*, 585−598.
19. Dumas, J. J., Zhu, Z., Connolly, J. L., and Lambright, D. G. (1999) *Structure 7*, 413−423.
20. Esters, H., Alexandrov, K., Constantinescu, A. T., Goody, R. S., and Scheidig, A. J. (2000) *J. Mol. Biol. 298*, 111−121.
21. Ullrich, O., Stenmark, H., Alexandrov, K., Huber, L. A., Kaibuchi, K., Sasaki, T., Takai, Y., and Zerial, M. (1993) *J. Biol. Chem. 268*, 18143−18150.
22. Martincic, I., Peralta, M. E., and Ngsee, J. K. (1997) *J. Biol. Chem. 272*, 26991−26998.
23. Dirac-Svejstrup, A. B., Sumizawa, T., and Pfeffer, S. R. (1997) *EMBO J. 16*, 465−472.
24. Burton, J. L., Slepnev, V., and De Camilli, P. V. (1997) *J. Biol. Chem. 272*, 3663−3668.
25. Yang, X., Matern, H. T., and Gallwitz, D. (1998) *EMBO J. 17*, 4954−4963.
26. Brennwald, P., and Novick, P. (1993) *Nature 362*, 560−563.
27. Stenmark, H., Valencia, A., Martinez, O., Ullrich, O., Goud, B., and Zerial, M. (1994) *EMBO J. 13*, 575−583.
28. Ostermeier, C., and Brunger, A. T. (1999) *Cell 96*, 363−374.
29. Merithew, E., Hatherly, S., Dumas, J. J., Lawe, D. C., Heller-Harrison, R., and Lambright, D. G. (2001) *J. Biol. Chem. 276*, 13982−13988.
30. Pereira-Leal, J. B., and Seabra, M. C. (2000) *J. Mol. Biol. 301*, 1077−1087.
31. Burton, J. L., Burns, M. E., Gatti, E., Augustine, G. J., and De Camilli, P. (1994) *EMBO J. 13*, 5547−5558.
32. Zhu, Z., Dumas, J. J., Lietzke, S. E., and Lambright, D. G. (2001) *Biochemistry 40*, 3027−3036.
33. Walch-Solimena, C., Collins, R. N., and Novick, P. J. (1997) *J. Cell Biol. 137*, 1495−1509.
34. Collins, R. N., Brennwald, P., Garrett, M., Lauring, A., and Novick, P. (1997) *J. Biol. Chem. 272*, 18281−18289.
35. Nuoffer, C., Wu, S. K., Dascher, C., and Balch, W. E. (1997) *Mol. Biol. Cell 8*, 1305−1316.
36. Muller-Pillasch, F., Zimmerhackl, F., Lacher, U., Schultz, N., Hameister, H., Varga, G., Friess, H., Buchler, M., Adler, G., and Gress, T. M. (1997) *Genomics 46*, 389−396.
37. Burstein, E. S., Brondyk, W. H., and Macara, I. G. (1992) *J. Biol. Chem. 267*, 22715−22718.
38. Brondyk, W. H., McKiernan, C. J., Burstein, E. S., and Macara, I. G. (1993) *J. Biol. Chem. 268*, 9410−9415.
39. Yu, H., and Schreiber, S. L. (1995) *Nature 376*, 788−791.
40. Press, W. H., Flannery, B. P., Teukolsky, S. A., and Vetterling, W. T. (1986) *Numerical Recipes*, Cambridge University Press, Cambridge.
41. Kawashima, T., Berthet-Colominas, C., Wulff, M., Cusack, S., and Leberman, R. (1996) *Nature 379*, 511−518.
42. Boriack-Sjodin, P. A., Margarit, S. M., Bar-Sagi, D., and Kuriyan, J. (1998) *Nature 394*, 337−343.
43. Goldberg, J. (1998) *Cell 95*, 237−248.
44. Worthylake, D. K., Rossman, K. L., and Sondek, J. (2000) *Nature 408*, 682−688.
45. Renault, L., Kuhlmann, J., Henkel, A., and Wittinghofer, A. (2001) *Cell 105*, 245−255.
46. Day, G. J., Mosteller, R. D., and Broek, D. (1998) *Mol. Cell. Biol. 18*, 7444−7454.

BI0116792